20 November 1998

ELSEVIER

Chemical Physics Letters 297 (1998) 121–126

CHEMICAL PHYSICS LETTERS

Ion chemistry in octafluorocyclobutane, *c*-C_4F_8

C.Q. Jiao [a], A. Garscadden [b,*], P.D. Haaland [a]

[a] *Mobium Enterprises, 5100 Springfield Pike, Dayton, OH 45431-1231, USA*
[b] *AFRL / PR, Bldg 18A, 1950 Fifth St., Wright-Patterson Air Force Base, OH 45433-7251, USA*

Received 13 July 1998; in final form 24 September 1998

Abstract

Cross-sections for electron impact ionization of octafluorocyclobutane (*c*-C_4F_8) have been measured from 10 to 200 eV by Fourier transform mass spectrometry. No parent ion is observed, and over half of the dissociative ionization yields $C_2F_4^+$ and $C_3F_5^+$. Eleven other fluorocarbon cations are produced with smaller cross-sections, giving a total ionization cross-section of $(1.6 \pm 0.2) \times 10^{-15}$ cm^2 between 80 and 200 eV. Only CF_2^+ and $C_2F_3^+$ react further with the parent molecule to yield $C_3F_5^+$ as the primary product. No evidence of cationic polymerization was found. F^- and $C_4F_8^-$ are formed by electron attachment at energies below 10 eV, but neither reacts further with *c*-C_4F_8.

1. Introduction

Octafluorocyclobutane (*c*-C_4F_8) is a good high-voltage insulator, and the electron attachment to this molecule has been extensively studied [1–18]. *c*-C_4F_8 is also used as a reagent for reactive ion etching of semiconductors [19], where recent studies have shown that positive ions are intimately involved in the surface deposition and etching processes [20]. Early data on the ionization cross-section of this fluorocarbon at 35 eV [4] and 70 eV [21] have recently been updated with quadrupole mass spectrometry measurements by Sugai and co-workers [22]. The sensitivity of quadrupole instruments is inherently nonlinear with mass, so here we present a complete characterization of the partial ionization of *c*-C_4F_8 using Fourier transform mass spectrometry (FTMS) technique.

Although positive ion formation by electron impact in plasmas is essential to maintain the conductivity that characterizes the plasma state, the stoichiometry of ion species can be modified by charge transfer reactions before ions diffuse to the boundary and are extracted by electrostatic sheath fields. We therefore also present an investigation of the evolution of positive and negative ion composition that results from reactions of the dissociatively ionized fragments with the parent *c*-C_4F_8.

2. Experimental

Octafluorocyclobutane (99 + %, TCI America) is mixed with argon (99.999% Matheson Research Grade) with a ratio (*c*-C_4F_8:Ar) of 1:2, and admitted through a precision leak valve into a modified Extrel FTMS system that has been described in detail else-

* Corresponding author. Fax: +1 937 656 4657; E-mail: alan.garscadden@wl.wpafb.af.mil

0009-2614/98/$ - see front matter
PII: S0009-2614(98)01107-5

where [23]. Ions are formed by electron impact in a cubic ion cyclotron resonance (ICR) trap cell at pressures in the 10^{-7} Torr range. An electron gun (Kimball Physics ELG2, Wilton, NH) irradiates that trap for 6 ms with a few hundred picocoulombs of low-energy electrons. The motions of the ions are constrained radially by a superconducting solenoidal magnetic field (~ 2 T) and axially by a nominal electrostatic potential (1 V) applied to the trap faces that are perpendicular to the magnetic field. Ions of all mass-to-charge ratios are simultaneously and coherently excited into cyclotron orbits using a stored waveform [24,25] applied to two opposing trap faces that are parallel to the magnetic field. Following cyclotron excitation, the image currents induced on the two remaining faces of the trap are amplified, digitized, and Fourier analyzed to yield a mass spectrum.

Calculation of cross-sections from the mass spectrum intensities requires knowledge of the gas densities, the electron beam current, and the number or ions produced. These calibration issues have been described previously [23,25,26]. The intensity ratios of the ions from *c*-C_4F_8 to Ar^+ give cross-sections relative to those for argon ionization [27] since the *c*-C_4F_8:Ar pressure ratio is quantified by capacitance manometry of the gas mixture. The absolute *c*-C_4F_8 pressure at the ICR trap that is needed for ion–molecule kinetic analysis is inferred from the rate coefficient of the known reaction of O_2^+ with *c*-C_4F_8 [28].

The distribution of electron energies in the trap, based on the solution of Laplace's equation for the experimental geometry, is roughly Gaussian with a full width at half maximum of 0.5 eV due to the electrostatic trapping bias [23]. The mean energy of the irradiating electrons is accurate to ± 0.2 eV based on comparison of noble gas ionization thresholds with spectroscopic data. We fit the cross-section data to an empirical functional form using a limited number of parameters:

$$\sigma = A \tanh \frac{\pi(\varepsilon - T)}{\alpha} e^{-k(\varepsilon - T)},$$

where σ is the cross-section, ϵ is the electron energy, T is the appearance potential, A scales the amplitude, α quantifies $d\sigma/d\epsilon$ near threshold, and k characterizes the higher-energy behavior.

3. Results and discussion

Electron impact ionization of *c*-C_4F_8 produces thirteen ion species, with $C_2F_4^+$ and $C_3F_5^+$ comprising over half of the yield from the threshold to 200 eV. Other fragment ions include CF_x^+ and $C_2F_x^+$ with $x = 1$–3, $C_3F_y^+$ with $y = 1$–4, and F^+. The molecular ion, $C_4F_8^+$, is not found by electron im-

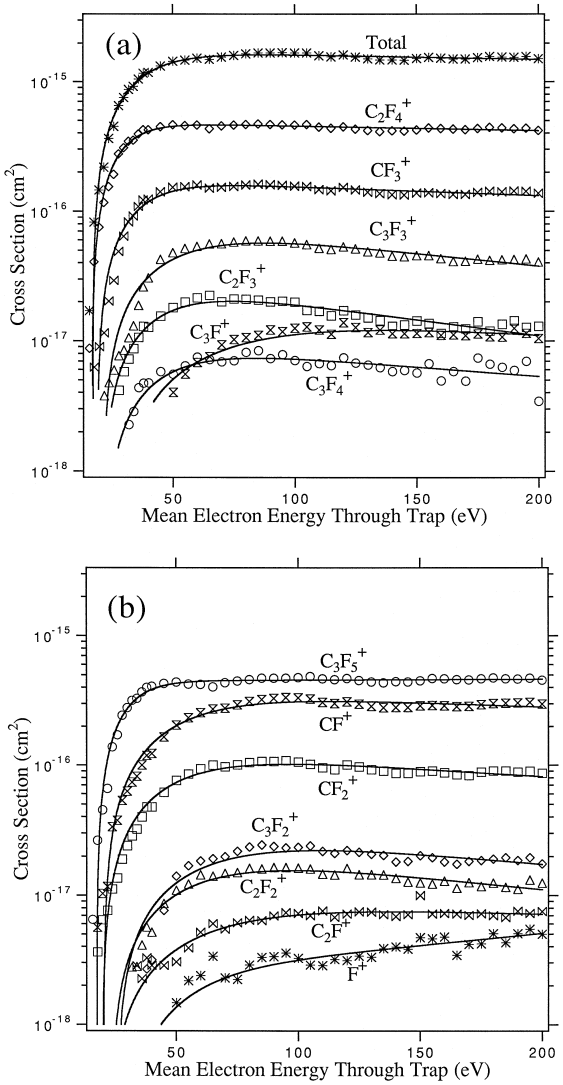

Fig. 1. (a) and (b): Cross-sections for ionization of *c*-C_4F_8 by electron impact. Points represent experimental data, and solid lines are fits of the equation described in the text.

pact. The total ionization cross-section reaches a maximum value of $(1.6 \pm 0.2) \times 10^{-15}$ cm^2 at 80 eV, and levels off thereafter. The cross-sections for each dissociative ionization process as a function of the electron energy are shown in Fig. 1 and the coefficients for our functional fit are summarized in Table 1. Data in Fig. 1 are compared to the previously reported findings, namely, the ionization cross-sections at 35 eV [4] and 70 eV [21] measured with magnetic mass spectrometers, and a recent quadrupole mass spectrometry measurement of the dissociative ionization [22]. There are significant differences in the dissociative ionization cross-sections among the data from these measurements including the present FTMS assessment. The quadrupole measurement by Sugai and co-workers [22] reports 6 ions while the FTMS measurement yields quantitative results for 13 species whose cross-sections exceed 10^{-18} cm^2. The FTMS technique is intrinsically independent of ion mass. The ions are not collected, rather their influence on the near-field antennae, which is a consequence only of their orbital motion and Maxwell's equations, is the measured quantity. Furthermore, the combination of low reagent pressures (10^{-7} Torr) and short observation times (ms) precludes modification of the ion ensemble by charge transfer collisions. Finally, the FTMS experiment setup lacks a proximal filament on which pyrolysis can produce new species that confound interpretation of the mass spectrum.

Table 1
Fitting parameters for dissociative ionization cross-sections. Ions are listed in the order of increasing mass. Also listed are the cross-sections at 70 eV, σ, in units of 10^{-16} cm^2

Ion	A (cm^2)	k (eV^{-1})	α (eV)	T (eV)	σ
F^+	2.4×10^{-18}	-4.2×10^{-3}	127	27.4	0.02
CF^+	3.7×10^{-16}	1.6×10^{-3}	146	20.4	2.8
C_2F^+	9.1×10^{-18}	1.4×10^{-3}	190	22.3	0.05
CF_2^+	1.3×10^{-16}	2.7×10^{-3}	138	19.8	0.97
C_3F^+	1.7×10^{-17}	2.7×10^{-3}	230	27.4	0.09
$C_2F_2^+$	2.4×10^{-17}	4.5×10^{-3}	166	23.4	0.15
CF_3^+	1.8×10^{-16}	1.6×10^{-3}	77	19.0	1.5
$C_3F_2^+$	3.4×10^{-17}	3.8×10^{-3}	177	25.7	0.20
$C_2F_3^+$	3.0×10^{-17}	5.6×10^{-3}	112	21.1	0.20
$C_3F_3^+$	8.5×10^{-17}	4.5×10^{-3}	140	21.4	0.56
$C_2F_4^+$	4.8×10^{-16}	8.0×10^{-4}	55	16.9	4.5
$C_3F_4^+$	9.6×10^{-18}	3.3×10^{-3}	111	21.9	0.07
$C_3F_5^+$	4.5×10^{-16}	-1.4×10^{-4}	56	17.5	4.3

Gas-phase reactions of the above positive ions with neutral c-C_4F_8 are studied by double resonance experiments. Each of the ions is isolated and the mass spectrum is recorded at programmed reaction times. Only CF_2^+ and $C_2F_3^+$ are found to react, yielding $C_3F_5^+$ as the major product ion, reactions (1)–(10).

$$CF_2^+ + c\text{-}C_4F_8 \rightarrow CF_3^+ + (C_4F_7)\ 14\% \quad (1)$$
$$\rightarrow C_2F_4^+ + (C_3F_6)\ 5\% \quad (2)$$
$$\rightarrow C_3F_3^+ + (C_2F_7)\ 2\% \quad (3)$$
$$\rightarrow C_3F_5^+ + (C_2F_5)\ 53\% \quad (4)$$
$$\rightarrow C_4F_6^+ + (CF_4)\ 6\% \quad (5)$$
$$\rightarrow C_4F_7^+ + (CF)\ 20\%, \quad (6)$$
$$C_2F_3^+ + c\text{-}C_4F_8 \rightarrow CF^+ + (C_5F_{10})\ 3\% \quad (7)$$
$$\rightarrow C_2F_4^+ + (C_4F_7)\ 7\% \quad (8)$$
$$\rightarrow C_3F_5^+ + (C_3F_6)\ 81\% \quad (9)$$
$$\rightarrow C_4F_7^+ + (C_2F_4)\ 9\%. \quad (10)$$

Formulae in the parentheses of the equations do not necessarily imply the actual neutral product composition. These reactions do not significantly change the overall ion composition of a c-C_4F_8 plasma, since the relative concentrations of the reactant ions, CF_2^+ and $C_2F_3^+$, are very small. Therefore, one can expect that $C_2F_4^+$ and $C_3F_5^+$ are the major ionic species reaching the surface from the plasma. Reactions of several selected rare-gas ions with c-C_4F_8 are also studied, with major product ions shown in reactions (11)–(16).

$$Ar^+ + c\text{-}C_4F_8 \rightarrow C_2F_4^+ + (C_2F_4) + Ar\ 50\% \quad (11)$$
$$\rightarrow C_3F_5^+ + (CF_3) + Ar\ 46\%, \quad (12)$$
$$Kr^+ + c\text{-}C_4F_8 \rightarrow C_2F_4^+ + (C_2F_4) + Kr\ 81\% \quad (13)$$
$$\rightarrow C_3F_5^+ + (CF_3) + Kr\ 16\%, \quad (14)$$
$$Xe^+ + c\text{-}C_4F_8 \rightarrow C_2F_4^+ + (C_2F_4) + Xe\ 46\% \quad (15)$$
$$\rightarrow C_3F_5^+ + (CF_3) + Xe\ 52\%. \quad (16)$$

Minor product ions (with $\sim$1% branching ratios) from Ar^+ reaction include F^+, CF^+, CF_3^+ and C_2F^+,

from Kr^+ reaction, F^+, CF_2^+ and C_2F^+, and from Xe^+ reaction, C_2F^+ and $C_4F_8^+$. Although no molecular ion is produced by electron impact, it is found as a minor product of charge transfer from Xe^+. The parent ion has an orbitally degenerate electronic structure and so is subject to the Jahn–Teller distortion. The energy liberated during distortion is too great for the molecular ion to remain bound, resulting in fragmentation forming mainly $C_2F_4^+$ and $C_3F_5^+$. The charge transfer reaction occurs over a much longer time scale, so that nuclear potential energy of the *c*-$C_4F_8^+$ can be shared with the departing Xe atom through the long-range Langevin potential. The result is stabilization of a distorted $C_4F_8^+$ ion that may or may not retain the cyclic structure.

Rate coefficients are obtained by fitting ordinary differential equations to the time varying ion distributions such as those shown in Fig. 2. Table 2 summarizes these coefficients for reactant ions formed by electron impact at 20, 35, and 50 eV. The rate coefficients are independent of the energy with which the reactant ion is formed within our experimental uncertainty. This implies that internal excitation of the reactant ion, if it occurs by energetic electron impact, does not change the charge transfer kinetics.

Table 2
Ion–molecule reaction rate coefficients in units of 10^{-9} cm^3 s^{-1}, measured in three separate experiments, 1–3, in which the primary ions are formed by electron impact at 20, 35 and 50 eV, respectively

Reaction	Experiment 1	Experiment 2	Experiment 3
$CF_2^+ + C_4F_8$	–	0.47 ± 0.05	0.47 ± 0.05
$C_2F_3^+ + C_4F_8$	–	0.33 ± 0.05	0.30 ± 0.05
$Ar^+ + C_4F_8$	1.5 ± 0.2	1.3 ± 0.2	1.3 ± 0.2

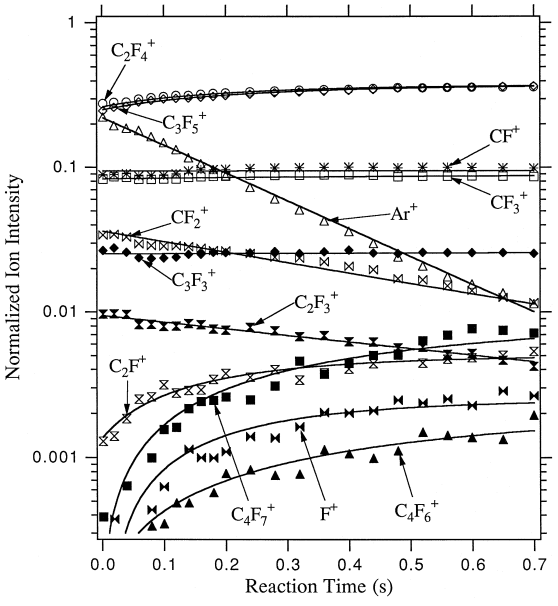

Fig. 2. Time evolution of positive ion species produced by 50 eV electron impact at a mixture of *c*-C_4F_8 and Ar (1:2) with a total pressure of 3.3×10^{-7} Torr. Data are shown only for the ions whose intensities change as the time. Points represent experimental data, and solid lines are fits of a kinetic model which gives the reaction rate coefficients presented in Table 2.

Attachment is not probed by beam electrons in our FTMS instrument because space-charge limits propagation of low energy electron beams along the 1 m path from the electron gun to the ion trap. Instead, we use the secondary electrons that are produced by ionization of the reagent gases and are trapped in the ICR cell along with negative ions. In experiments, a 50 eV electron beam irradiates the ion trap for an extended period (80 ms). The secondary electrons produced at different locations along the trapping axis of the cell are born with different electrostatic potential energies. These electrons un-

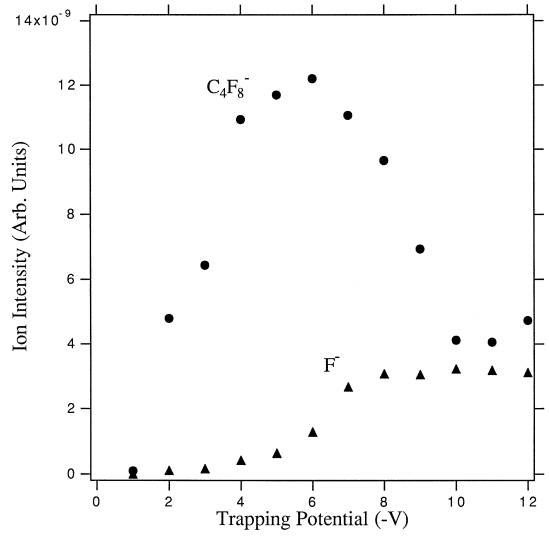

Fig. 3. Negative ion yields from trapped secondary electrons as a function of the applied trapping potential. The primary electron energy is 50 eV, and the electron beam period is 80 ms.

dergo damped harmonic motion in the trapping potential, where the damping arises from electron–neutral collisions with reagent gas. As the electrons cascade down in energy they have an opportunity to attach as well as be cooled by momentum transfer. Increasing the magnitude of the trapping potential increases the initial potential energy at which the secondary electrons are formed, so that processes with successively higher thresholds may be probed. Although this approach lacks the energy resolution of crossed beam measurements, it has the advantage that further reactions between anionic products of attachment and the parent gas may be conveniently probed. Fig. 3 shows the negative ion yield as a function of trapping potential for attachment to *c*-C_4F_8. Previous reports found a resonance for *c*-$C_4F_8^-$ peaking at 0.45 eV [8] and multiple resonance peaks for F^- at ~ 5 eV and higher energies [2,8]. Our data in Fig. 3 are qualitatively consistent with these findings. Production of F^- from *c*-C_4F_8 is a classic illustration of dissociative electron attachment, and has been extensively reported [2–4,9,14]. The observation of $C_4F_8^-$ at the low pressures ($< 10^{-6}$ Torr) and long experiment times (up to 1 s) of FTMS is more unusual, since there are no departing fragments to satisfy energy conservation in the exit channel leading to a single anion. While emission of infrared photons may stabilize the association product, one of the ring bonds in *c*-$C_4F_8^-$ may be broken while retaining the stoichiometry of the parent molecule. No reaction is found between either $C_4F_8^-$ or F^- and neutral *c*-C_4F_8, which exclude the possibility that $C_4F_8^-$ is formed by the reaction of F^- with *c*-C_4F_8 during the extended electron beam period.

4. Conclusions

Thirteen positive ions are produced by electron impact on *c*-C_4F_8 with $C_2F_4^+$ and $C_3F_5^+$ to be the predominant fragment ions and a total ionization cross-section of $(1.6 \pm 0.2) \times 10^{-15}$ cm^2 between 80 and 200 eV. No parent molecular ion $C_4F_8^+$ is observed. Relaxation of the ion composition by charge transfer reactions implies that ion fluxes will be comprised mainly of $C_2F_4^+$ and $C_3F_5^+$ under many plasma conditions. No evidence of cationic polymerization to form heavier ions was identified. Two negative ions are observed to form following impact of electrons with less than 10 eV of energy. F^- arises from standard dissociative attachment, while the formation of $C_4F_8^-$ involves either emission of a photon or stabilization by ring-opening. Neither F^- nor $C_4F_8^-$ reacts with *c*-C_4F_8.

Acknowledgements

The authors wish to acknowledge the Air Force Office of Scientific Research for supporting this research.

References

[1] A.A. Christodoulides, L.G. Christophorou, R.Y. Pai, C.M. Tung, J. Chem. Phys. 70 (1979) 1156.
[2] I. Sauers, L.G. Christophorou, J.G. Carter, J. Chem. Phys. 71 (1979) 3016.
[3] R.M. Reese, V.H. Dibeler, F.L. Mohler, J. Res. Natl. Bur. Stand. 57 (1956) 367.
[4] M.M. Bibby, G. Carter, Trans. Faraday Soc. 59 (1963) 2455.
[5] M.V. Kurepa, 3rd Czech. Conf. on Electronics and Vacuum Physics Transactions 107 (1965).
[6] R. Grajower, C. Lifshitz, Isr. J. Chem. 6 (1968) 847.
[7] W.T. Naff, C.D. Cooper, J. Chem. Phys. 49 (1968) 2784.
[8] P.W. Harland, J.C.J. Thynne, Int. J. Mass Spectrom. Ion Phys. 10 (1972) 11.
[9] C. Lifshitz, R. Grajower, Int. J. Mass Spectrom. Ion Phys. 10 (1972) 25.
[10] K.M. Bansal, R.W. Fessenden, J. Chem. Phys. 59 (1973) 1760.
[11] F.J. Davis, R.N. Compton, D.R. Nelson, J. Chem. Phys. 59 (1973) 2324.
[12] L.G. Christophorou, D.L. McCorkle, D. Pittman, J. Chem. Phys. 60 (1974) 1183.
[13] P.W. Harland, J.L. Franklin, J. Chem. Phys. 61 (1974) 1621.
[14] R.L. Woodin, M.S. Foster, J.L. Beauchamp, J. Chem. Phys. 72 (1980) 4223.
[15] L.G. Christophorou, R.A. Mathis, D.R. James, D.L. McCorkle, J. Phys. D: Appl. Phys. 14 (1981) 1889.
[16] S.M. Spyrou, S.R. Hunter, L.G. Christophorou, J. Chem. Phys. 83 (1985) 641.
[17] A.A. Christodoulides, L.G. Christophorou, D.L. McCorkle, Chem. Phys. Lett. 139 (1987) 350.
[18] T.M. Miller, R.A. Morris, A.E.S. Miller, A.A. Viggiano, J.F. Paulson, Int. J. Mass Spectrom. Ion Process. 135 (1994) 195.
[19] H. Kazumi, K. Tago, Jpn. J. Appl. Phys. 34 (1995) 2125.
[20] Y. Gotoh, T. Kure, Jpn. J. Appl. Phys. 34 (1995) 2132.
[21] J.A. Beran, L. Kevan, J. Phys. Chem. 73 (1969) 3866.
[22] H. Toyoda, M. Iio, H. Sugai, Jpn. J. Appl. Phys. 36 (1997) 3730.

[23] K. Riehl, Collisional detachment of negative ions using FTMS, Ph.D. Thesis, Air Force Inst. Technol., Wright-Patterson AFB, OH, 1992.
[24] A.G. Marshall, T.L. Wang, T.L. Ricca, J. Am. Chem. Soc. 107 (1985) 7893.
[25] S. Guan, J. Chem. Phys. 91 (1989) 775.
[26] P.D. Haaland, Chem. Phys. Lett. 170 (1990) 146.
[27] R.C. Wetzel, F.A. Baioochi, T.R. Hayes, R.S. Freund, Phys. Rev. 35 (1987) 559.
[28] R.A. Morris, T.M. Miller, A.A. Viggiano, J.F. Paulson, J. Geophys. Res. 100 (1995) 1287.